Supplementary Information

Controlling Pt Nanoparticle Sintering by Sub-Monolayer MgO ALD Thin Films

Zhiwei Zhang,[a] Matthias Filez,[a,b] Eduardo Solano,[c] Nithin Poonkottil,[a] Jin Li,[a] Matthias M. Minjauw,[a] Hilde Poelman,[d] Martin Rosenthal,[e] Philipp Brüner,[f] Vladimir V. Galvita,[d] Christophe Detavernier,[a] Jolien Dendooven*[a]

[a] Z. Zhang, Dr. M. Filez, Dr N. Poonkottil, Dr. J. Li, Dr. M. M. Minjauw, Prof. C. Detavernier, Prof. J. Dendooven
Conformal Coating of Nanomaterials (CoCooN)
Department of Solid State Sciences
Ghent University
Krijgslaan 281/S1, 9000 Ghent (Belgium)
* e-mail: Jolien.Dendooven@UGent.be

[b] Dr. M. Filez
Centre for Membrane Separations Adsorption Catalysis and Spectroscopy for Sustainable Solutions (cMACS)
KU Leuven
Celestijnenlaan 200F, 3001 Leuven (Belgium)

[c] Dr. E. Solano
NCD-SWEET beamline
ALBA synchrotron light source
Carrer de la Llum 2-26, 08290, Cerdanyola del Vallès (Spain)

[d] Laboratory for Chemical Technology
Ghent University
Technologiepark 125, 9052 Ghent (Belgium)

[e] Dr. M. Rosenthal
DUBBLE beamline
ESRF - The European Synchrotron
71 Avenue des Martyrs, 38000 Grenoble (France)

[f] P. Brüner
IONTOF Technologies GmbH
Heisenbergstr. 15, 48149 Muenster (Germany)

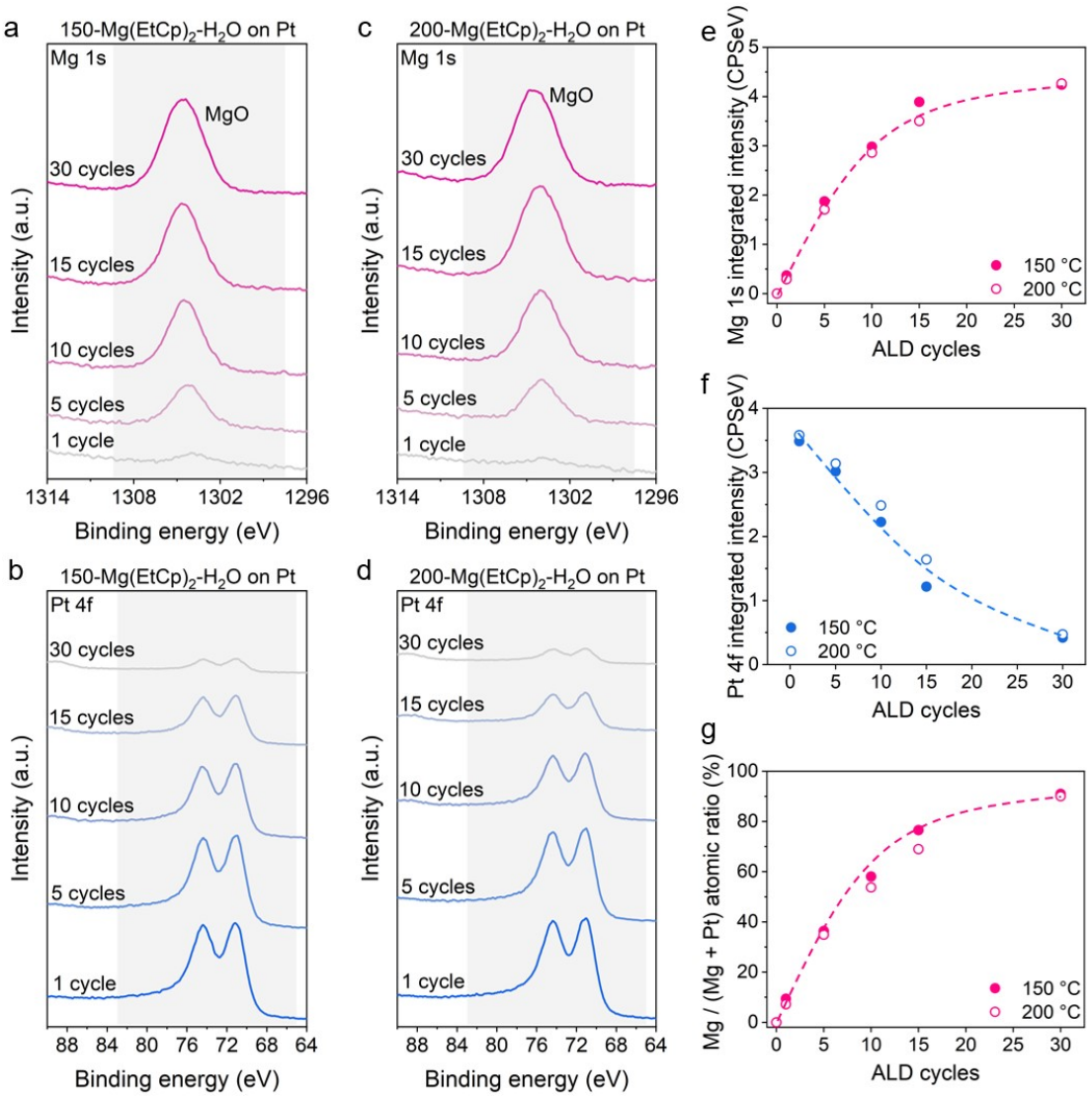

Figure S1. XPS spectra recorded after 1, 5, 10, 15 and 30 ALD cycles of the $Mg(EtCp)_2$-H_2O process on a sputtered Pt substrate. The binding energy scale is calibrated by taking Pt $4f_{5/2}$ at 70.9 eV. The background type is Tougaard for Mg 1s and Shirley for Pt 4f, respectively. (a) Mg 1s and (b) Pt 4f spectra for the samples prepared at 150 °C. (c) Mg 1s and (d) Pt 4f spectra for the samples prepared at 200 °C. (e) Mg 1s peak intensity integrated in the region from 1310 eV to 1298 eV and (f) Pt 4f peak intensity integrated in the region from 83 eV to 65 eV as a function of the number of ALD cycles for both deposition temperatures. (g) Mg atomic fraction as a function of the number of ALD cycles for both deposition temperatures. The dashed lines serve as guides to the eye. The Mg atomic fraction is determined by dividing the peak area of the Mg 1s signal by the summed areas of the Mg 1s and Pt 4f signals, taking into account the relative sensitivity factors of both photoemission peaks.

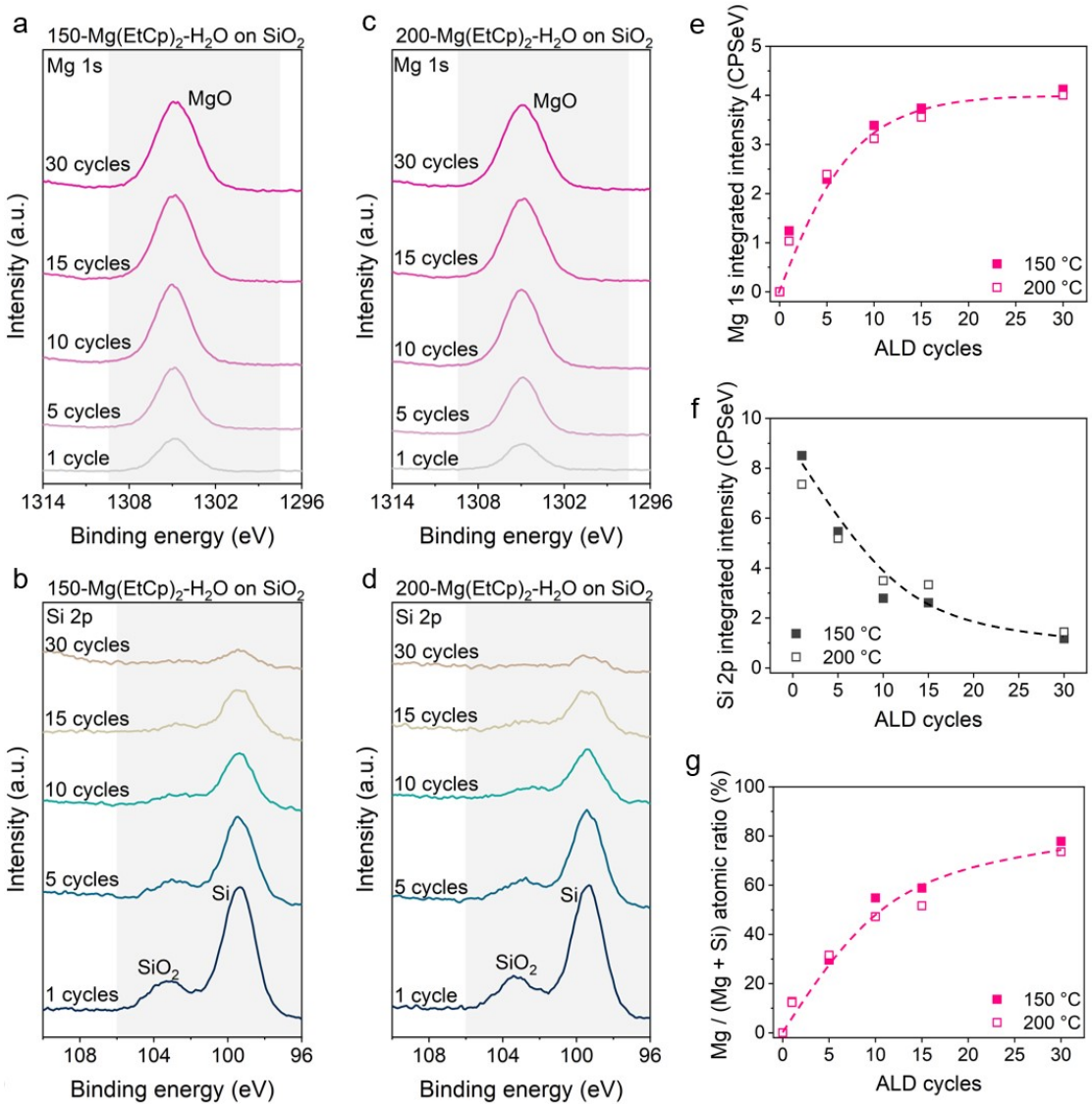

Figure S2. XPS spectra recorded after 1, 5, 10, 15 and 30 ALD cycles of the $Mg(EtCp)_2$-H_2O process on a native SiO_2 substrate. The binding energy scale is calibrated by taking Si $2p_{3/2}$ at 99.4 eV. The background type is Tougaard for Mg 1s and Linear for Si 2p, respectively. (a) Mg 1s and (b) Si 2p spectra for the samples prepared at 150 °C. (c) Mg 1s and (d) Si 2p spectra for the samples prepared at 200 °C. (e) Mg 1s peak intensity integrated in the region from 1310 eV to 1298 eV and (f) Si 2p peak intensity integrated in the region from 106 eV to 96 eV as a function of the number of ALD cycles for both deposition temperatures. (g) Mg atomic fraction as a function of the number of ALD cycles for both deposition temperatures. The dashed lines serve as guides to the eye. The Mg atomic fraction is determined by dividing the peak area of the Mg 1s signal by the summed areas of the Mg 1s and Si 2p signals, taking into account the relative sensitivity factors of both photoemission peaks.

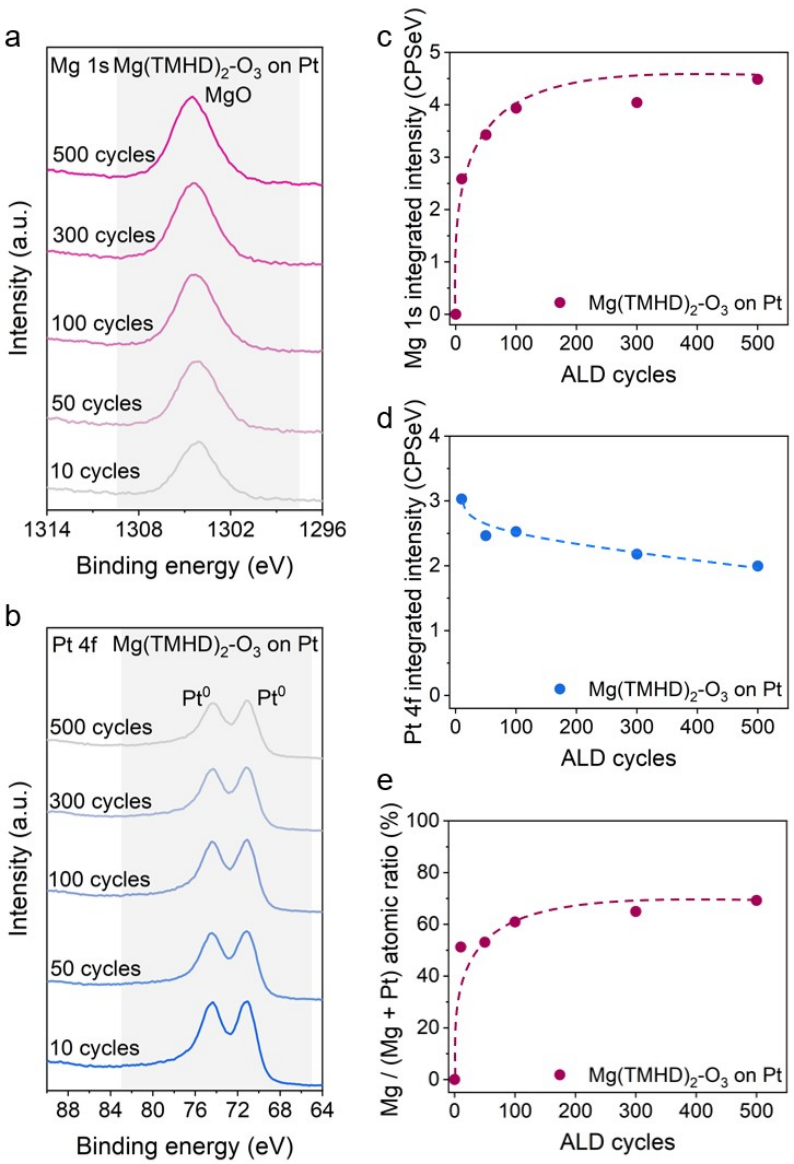

Figure S3. XPS spectra recorded after 10, 50, 100, 300 and 500 ALD cycles of the $Mg(TMHD)_2$-O_3 process at 250 °C on sputtered Pt substrate. The binding energy scale is calibrated by taking Pt $4f_{5/2}$ at 70.9 eV. The background type is Tougaard for Mg 1s and Shirley for Pt 4f, respectively. (a) Mg 1s and (b) Pt 4f spectra. (c) Mg 1s peak intensity integrated in the region from 1310 eV to 1298 eV and (d) Pt 4f peak intensity integrated in the region from 83 eV to 65 eV as a function of the number of ALD cycles. (e) Mg atomic fraction as a function of the number of ALD cycles. The dashed lines serve as guides to the eye. The Mg atomic fraction is determined by dividing the peak area of the Mg 1s signal by the summed areas of the Mg 1s and Pt 4f signals, taking into account the relative sensitivity factors of both photoemission peaks.

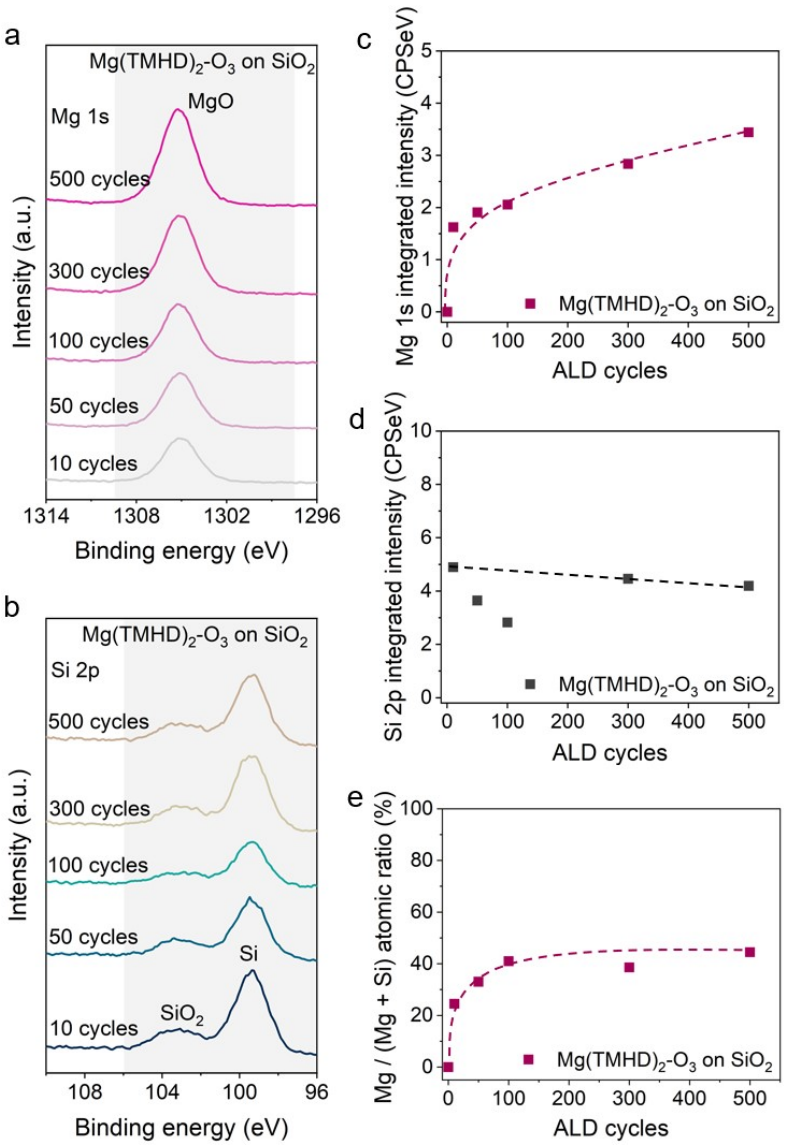

Figure S4. XPS spectra recorded after 10, 50, 100, 300 and 500 ALD cycles of the $Mg(TMHD)_2$-O_3 process at 250 °C on native SiO_2 substrate. The binding energy scale is calibrated by taking Si $2p_{3/2}$ at 99.4 eV. The background type is Tougaard for Mg 1s and Linear for Si 2p, respectively. (a) Mg 1s and (b) Si 2p spectra. (c) Mg 1s peak intensity integrated in the region from 1310 eV to 1298 eV and (d) Si 2p peak intensity integrated in the region from 106 eV to 96 eV as a function of the number of ALD cycles. (e) Mg atomic fraction as a function of the number of ALD cycles. The dashed lines serve as guides to the eye. The Mg atomic fraction is determined by dividing the peak area of the Mg 1s signal by the summed areas of the Mg 1s and Si 2p signals, taking into account the relative sensitivity factors of both photoemission peaks.

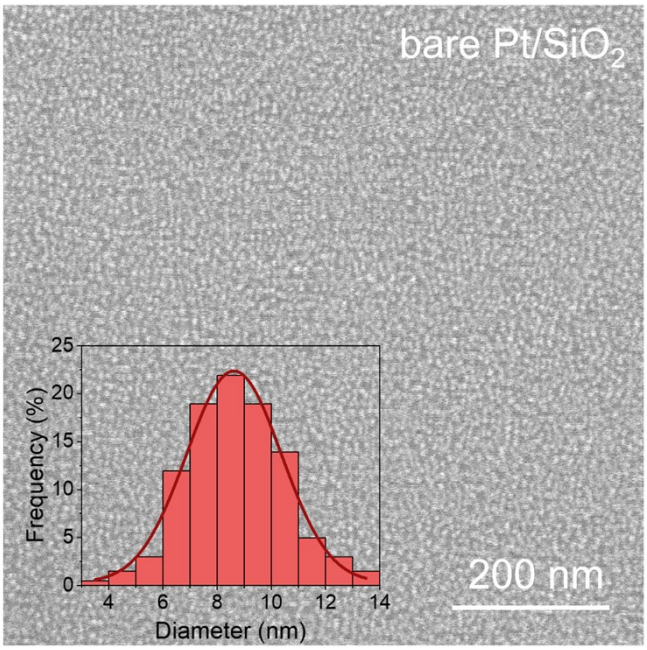

Figure S5. SEM image of Pt NPs on a native SiO_2 substrate, prepared by 25 ALD cycles of the $MeCpPtMe_3/O_2$ process at 300 °C. This sample is labeled as bare Pt/SiO_2 throughout the manuscript. The contrast and brightness of the image is optimized using the *ImageJ* software. A region with ca. 200 particles is selected and their sizes are measured and represented in a size distribution diagram (the inset).

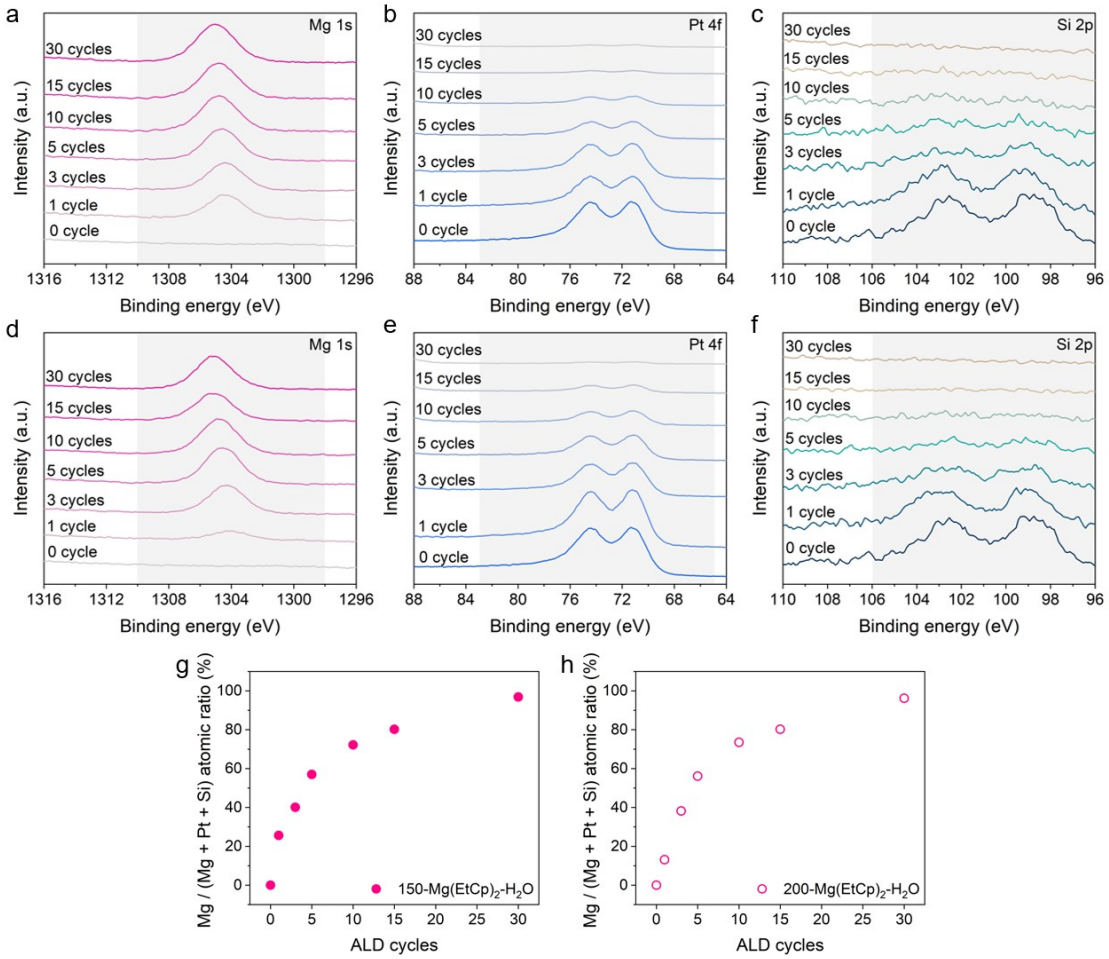

Figure S6. XPS spectra recorded after 0, 1, 3, 5, 10, 15 and 30 ALD cycles of the $Mg(EtCp)_2$-H_2O process on Pt/SiO_2. The binding energy scale is calibrated by taking Pt $4f_{5/2}$ at 70.9 eV. The background type is Tougaard for Mg 1s, Shirley for P4 4f and Linear for Si 2p, respectively. Mg 1s peak intensity is integrated in the region from 1310 eV to 1298 eV. Pt 4f peak intensity is integrated in the region from 83 eV to 65 eV. Si 2p peak intensity integrated in the region from 106 eV to 96 eV. (a) Mg 1s, (b) Pt 4f and (c) Si 2p spectra for the samples prepared at 150 °C. (d) Mg 1s, (e) Pt 4f and (f) Si 2p spectra for the samples prepared at 200 °C. (g,h) Mg atomic fraction as a function of the number of ALD cycles for both deposition temperatures: (g) 150 °C and (h) 200 °C. The Mg atomic fraction is determined by dividing the peak area of the Mg 1s signal by the summed areas of the Mg 1s, Pt 4f and Si 2p signals, taking into account the relative sensitivity factors of the three photoemission peaks.

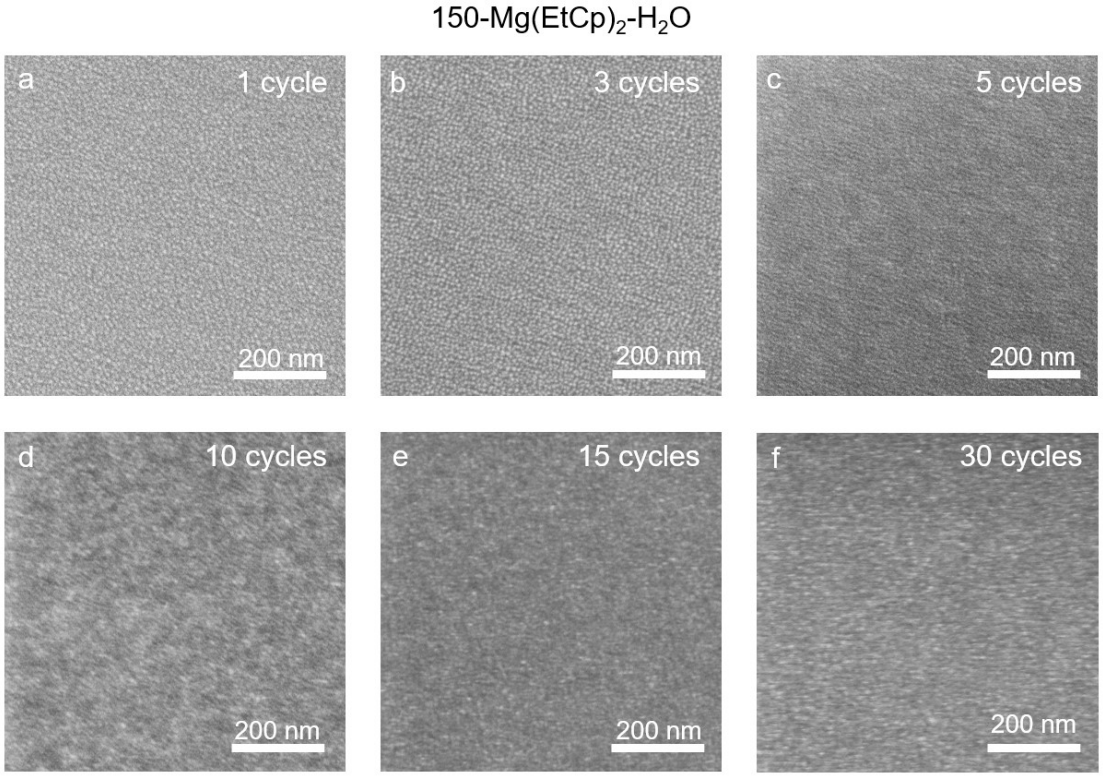

Figure S7. SEM images of Pt/SiO_2 overcoated with MgO using (a) 1, (b) 3, (c) 5, (d) 10, (e) 15 and (f) 30 ALD cycles of the $Mg(EtCp)_2$-H_2O process at 150 °C.

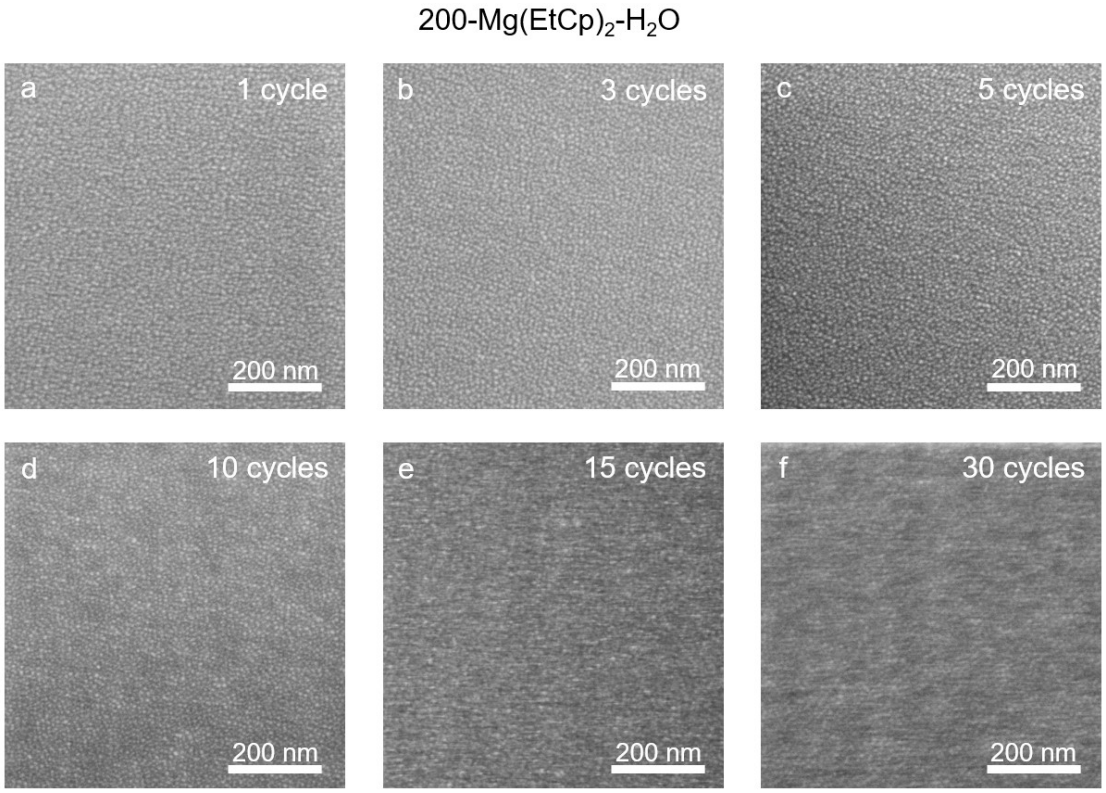

Figure S8. SEM images of Pt/SiO_2 overcoated with MgO using (a) 1, (b) 3, (c) 5, (d) 10, (e) 15 and (f) 30 ALD cycles of the $Mg(EtCp)_2$-H_2O process at 200 °C.

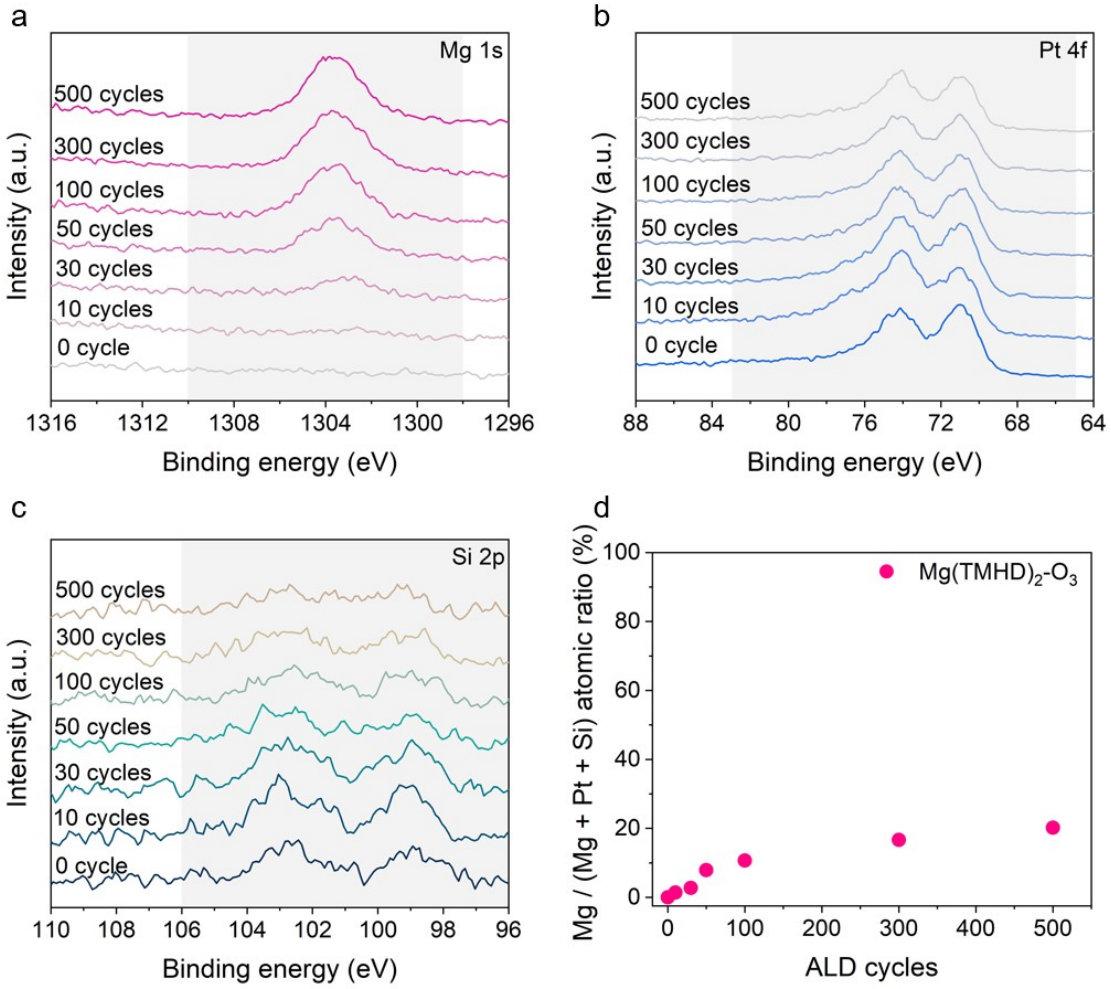

Figure S9. XPS spectra recorded after 0, 10, 30, 50, 100, 300 and 500 ALD cycles of the $Mg(TMHD)_2$-O_3 process at 250 °C on Pt/SiO_2. The binding energy scale is calibrated by taking Pt $4f_{5/2}$ at 70.9 eV. The background type is Tougaard for Mg 1s, Shirley for P4 4f and Linear for Si 2p, respectively. Mg 1s peak intensity is integrated in the region from 1310 eV to 1298 eV. Pt 4f peak intensity is integrated in the region from 83 eV to 65 eV. Si 2p peak intensity integrated in the region from 106 eV to 96 eV. (a) Mg 1s, (b) Pt 4f and (c) Si 2p spectra. (d) Mg atomic fraction as a function of the number of ALD cycles. The Mg atomic fraction is determined by dividing the peak area of the Mg 1s signal by the summed areas of the Mg 1s, Pt 4f and Si 2p signals, taking into account the relative sensitivity factors of the three photoemission peaks.

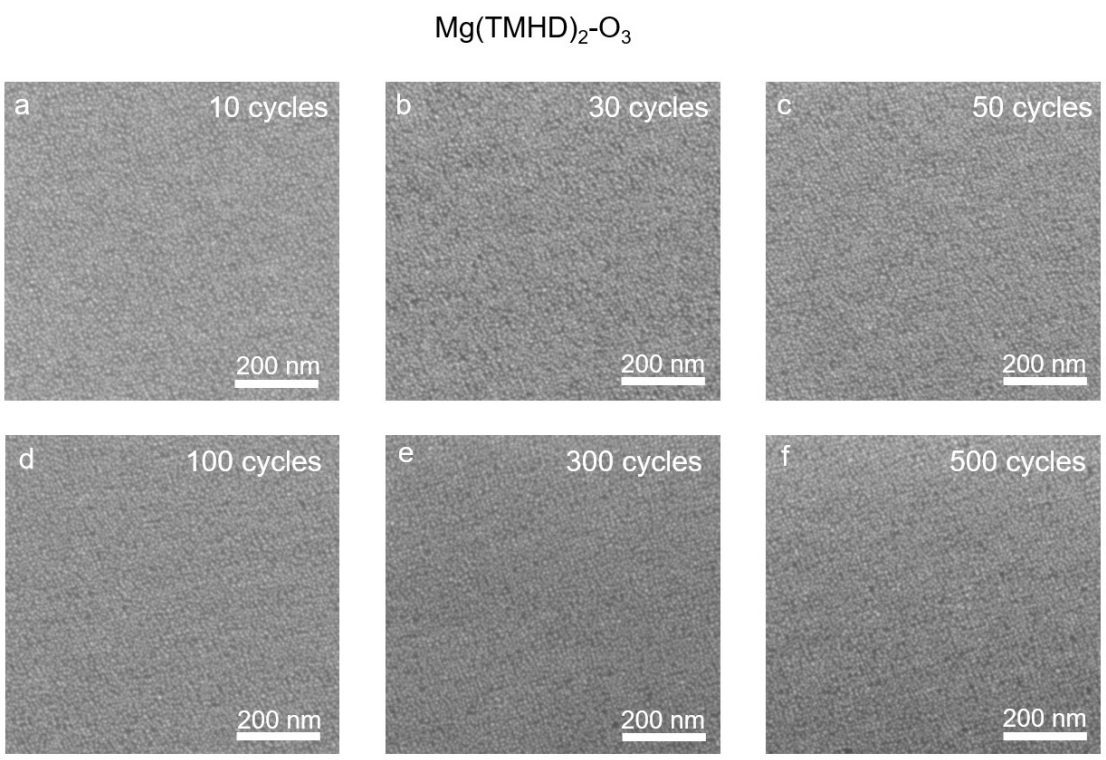

Figure S10. SEM images of Pt/SiO_2 overcoated with MgO using (a) 10, (b) 30, (c) 50, (d) 100, (e) 300 and (f) 500 ALD cycles of the $Mg(TMHD)_2$-O_3 process at 250 °C.

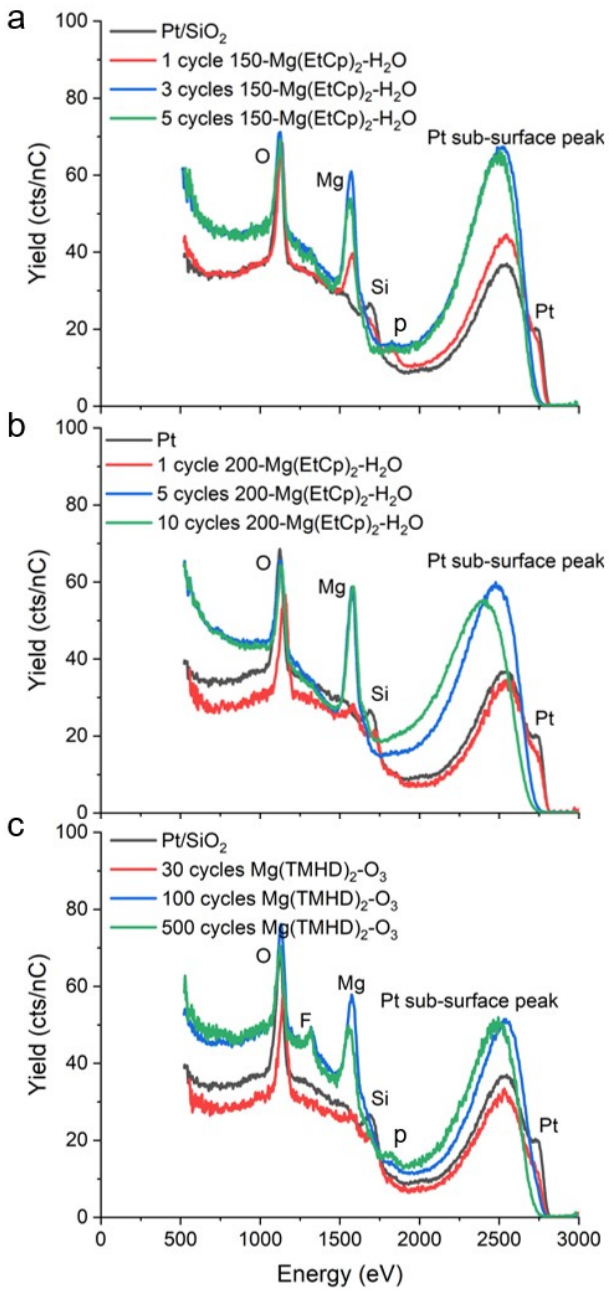

Figure S11. 3 keV He^+ LEIS spectra of Pt/SiO_2 without and with MgO overcoat, deposited with the $Mg(EtCp)_2$-H_2O ALD process at (a) 150 ℃ and (b) 200 ℃, and (c) with the $Mg(TMHD)_2$-O_3 process at 250 ℃.

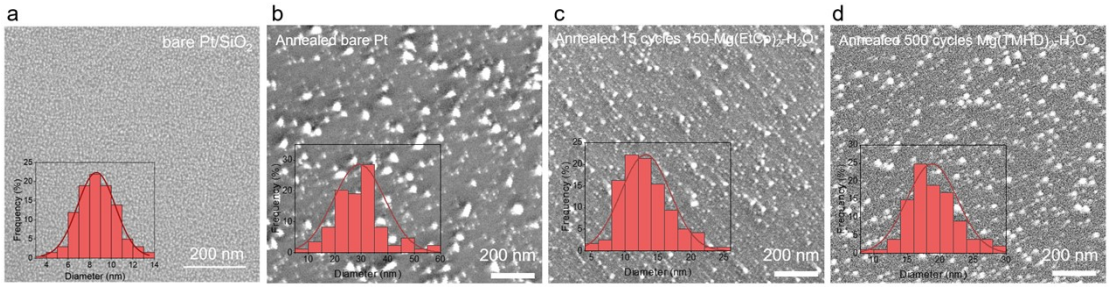

Figure S12. SEM images and corresponding size distribution diagrams of (a) bare Pt without annealing treatment, (b) bare Pt after 800 ℃ ramp annealing, (c) 15 cycles 150-$Mg(EtCp)_2$-H_2O after 800 ℃ ramp annealing and (d) 500 cycles $Mg(TMHD)_2$-O_3 after 800 ℃ ramp annealing.

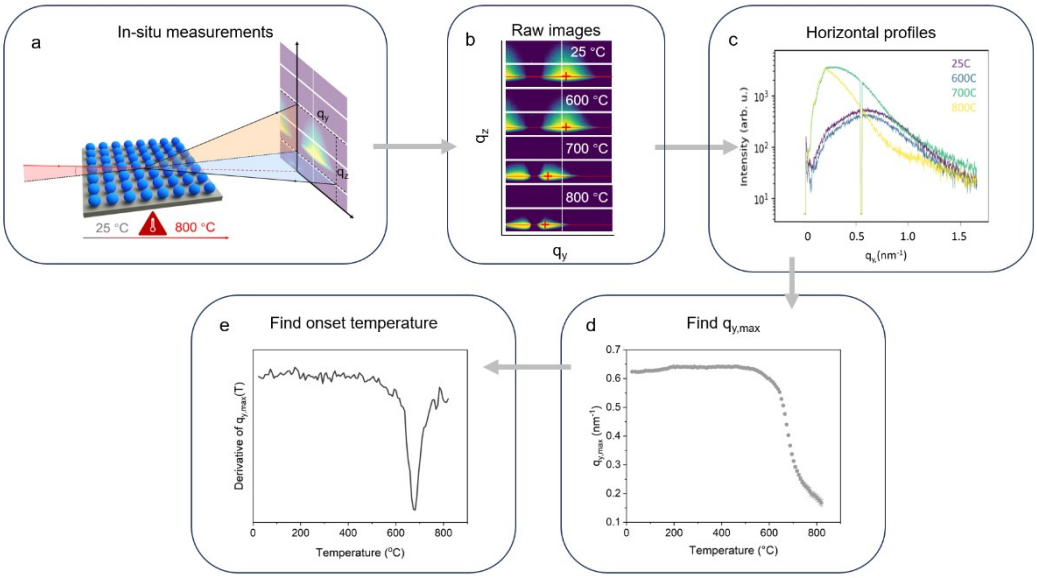

Figure S13. Schematic of the GISAXS geometry (a) and data analysis workflow (b-e). (b) Experimental 2D GISAXS patterns. (c) A 1D horizontal profile is extracted from the 2D image at the Si Yoneda peak (indicated by the red lines in (b)). (d) Fitting of a Gaussian function to the scattering peak in the 1D profiles yields the q_y position of the peak maximum, $q_{y,max}$, at each temperature. (e) The derivative of the $q_{y,max}$(temperature) curve shows a distinct minimum. The temperature at which this minimum occurs, is interpreted as the onset temperature for particle sintering.

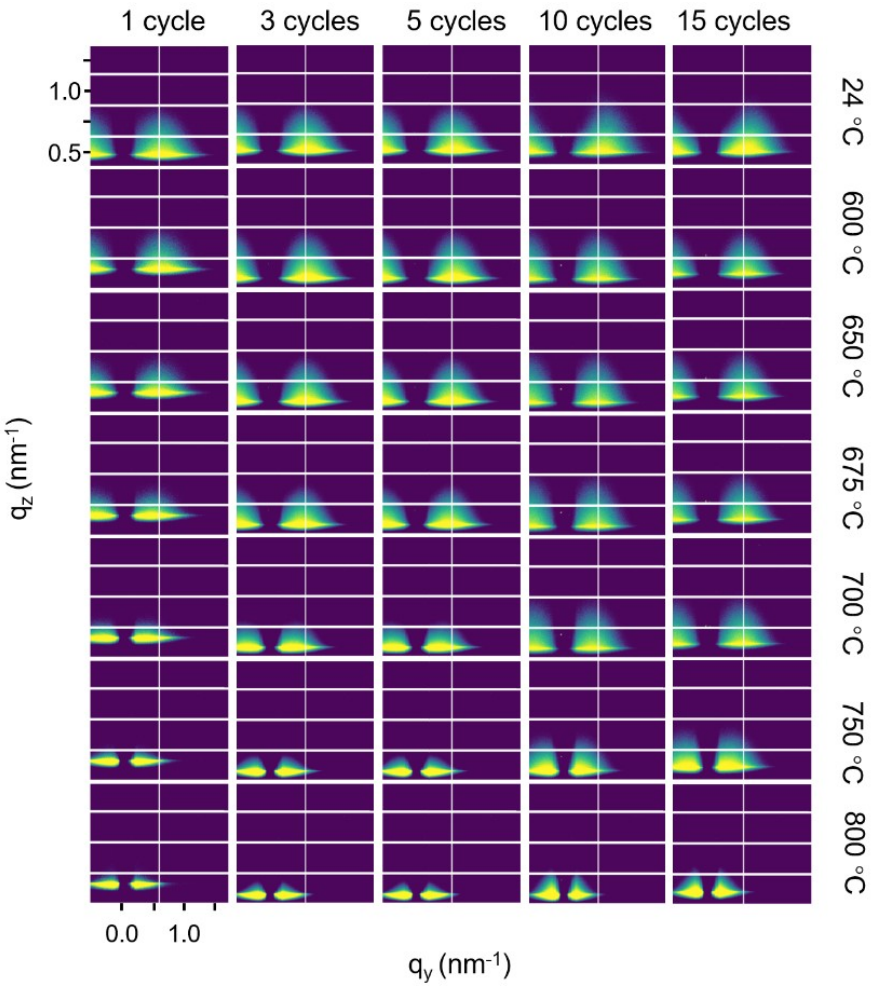

Figure S14. Selection of 2D GISAXS patterns recorded during in-situ O_2 anneals of Pt/SiO_2 with different MgO overlayers, prepared by 1, 3, 5, 10 and 15 $Mg(EtCp)_2$-H_2O ALD cycles at 150 °C, respectively. Going from top to bottom in the first column of the figure, the scattering features move closer together and the intensity around $q_y = 0$ nm^{-1} increases, indicative of NP sintering with increasing temperature. With increasing number of ALD cycles, the movement of the scattering peaks is delayed to higher temperatures, implying a delay in sintering and hence enhanced thermal stability of the Pt NPs.

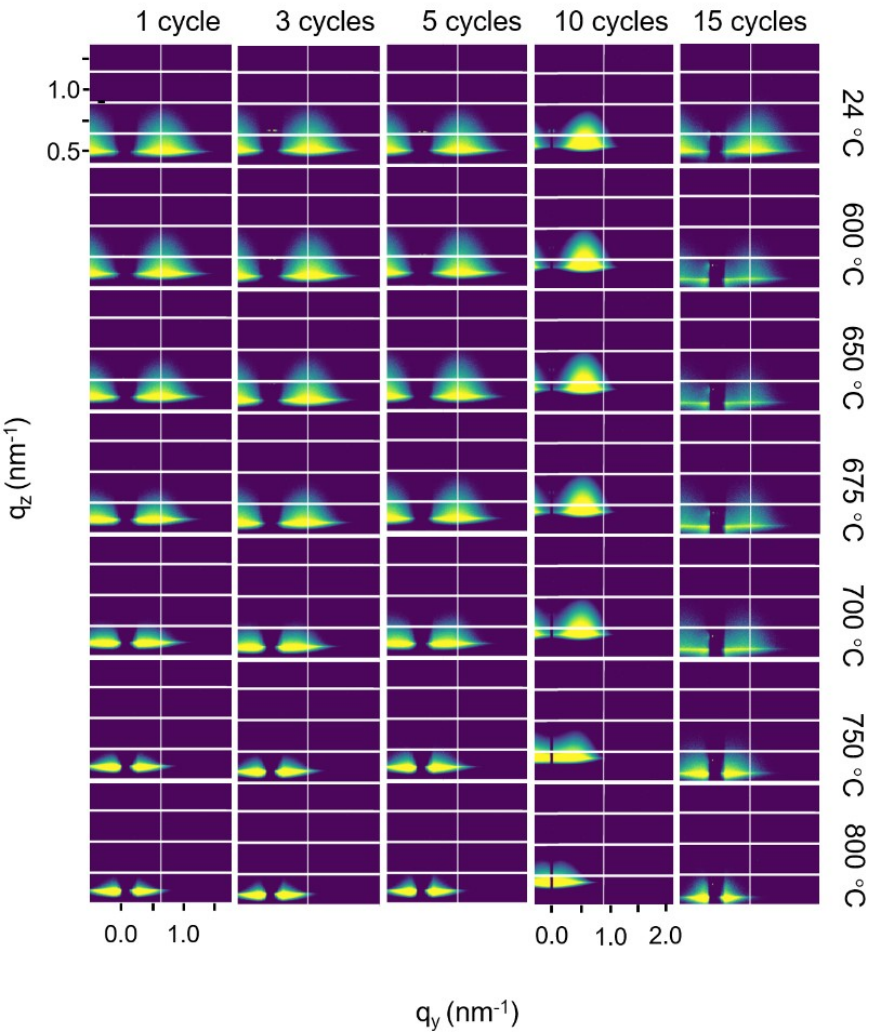

Figure S15. Selection of 2D GISAXS patterns recorded during in-situ O_2 anneals of Pt/SiO_2 with different MgO overlayers, prepared by 1, 3, 5, 10 and 15 Mg(EtCp)$_2$-H_2O ALD cycles at 200 °C, respectively. Going from top to bottom in the first column of the figure, the scattering features move closer together and the intensity around q_y = 0 nm^{-1} increases, indicative of NP sintering with increasing temperature. With increasing number of ALD cycles, the movement of the scattering peaks is delayed to higher temperatures, implying a delay in sintering and hence enhanced thermal stability of the Pt NPs.

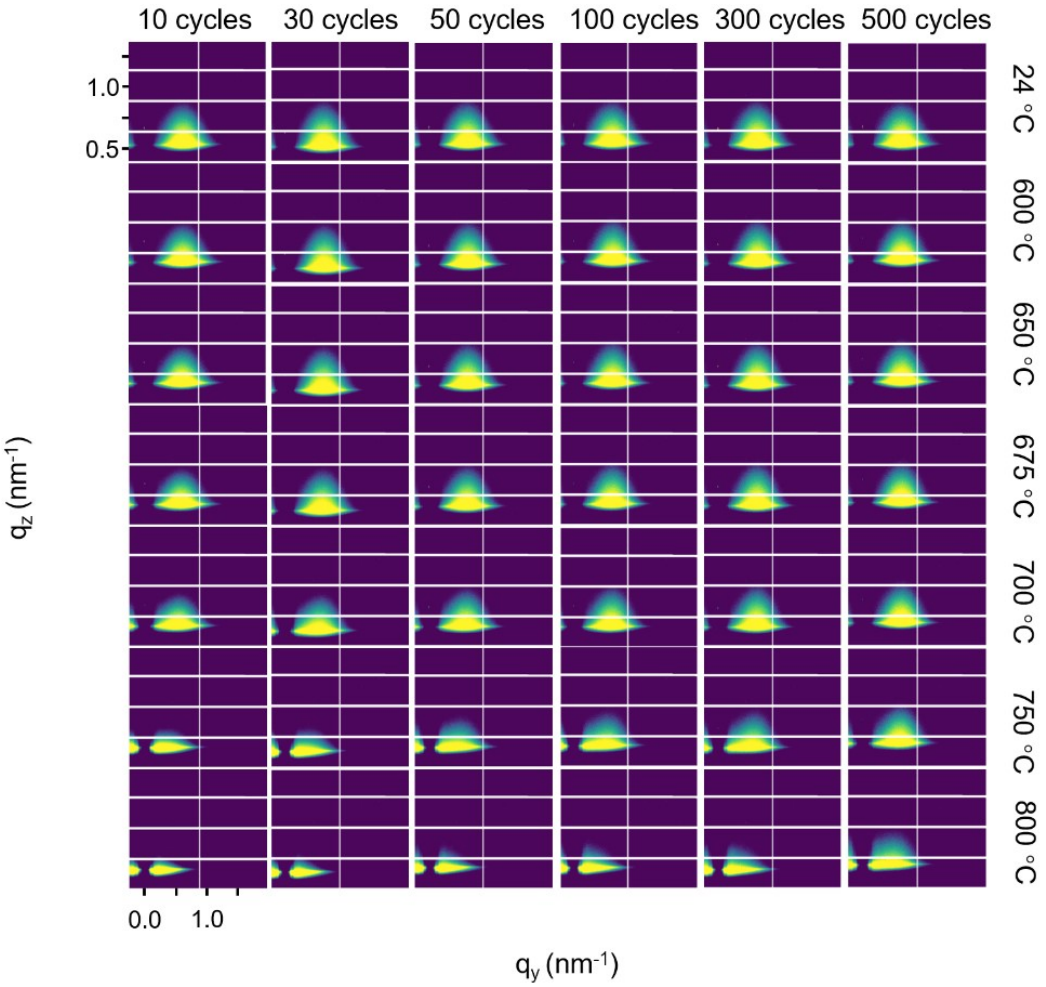

Figure S16. Selection of 2D GISAXS patterns recorded during in-situ O_2 anneals of Pt/SiO_2 with different MgO overlayers, prepared by 10, 30, 50, 100, 300 and 500 $Mg(TMHD)_2$-O_3 ALD cycles, respectively. Going from top to bottom in the first column of the figure, the scattering features move closer together and the intensity around q_y = 0 nm^{-1} increases, indicative of NP sintering with increasing temperature. With increasing number of ALD cycles, the movement of the scattering peaks is delayed to higher temperatures, implying a delay in sintering and hence enhanced thermal stability of the Pt NPs.

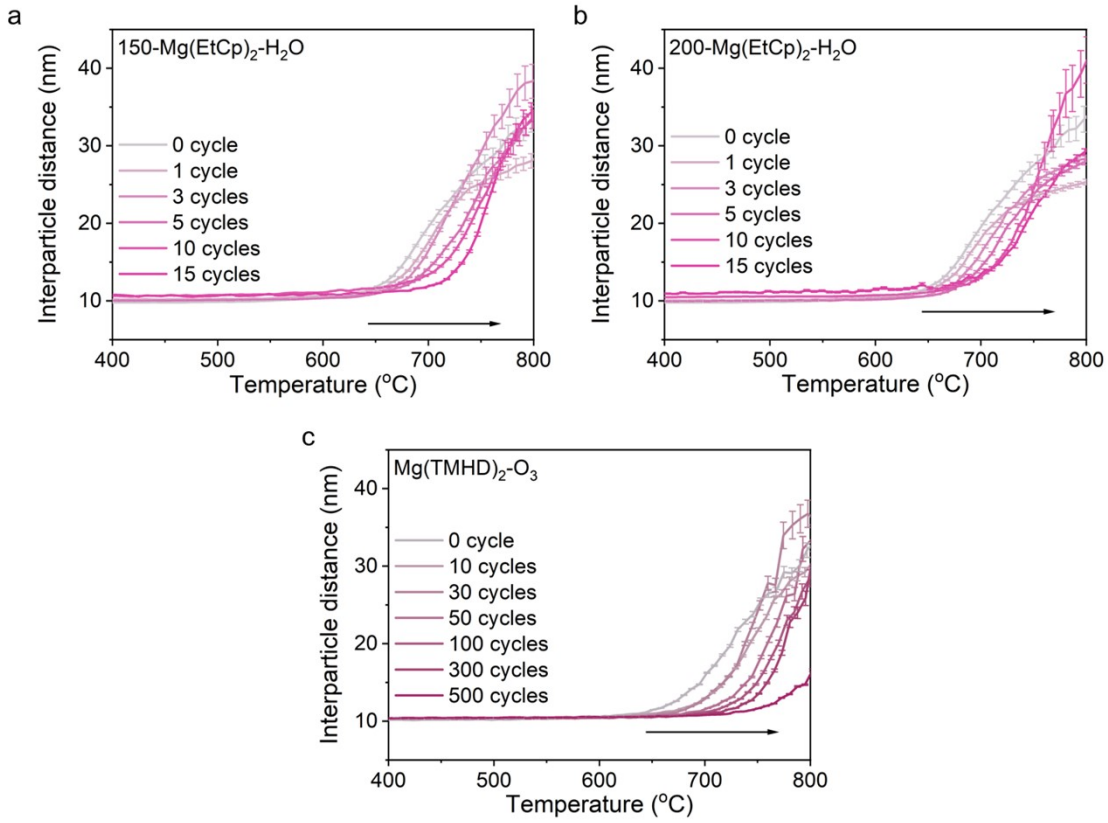

Figure S17. Evolution of the center-to-center NP distance with temperature in the range 400-800 °C during O_2 anneals of Pt/SiO_2 with different MgO overlayers, prepared by 1, 3, 5, 10 and 15 $Mg(EtCp)_2$-H_2O ALD cycles at (a) 150 °C and (b) 200 °C, and (c) Pt/SiO_2 with different MgO overlayers, prepared by 10, 30, 50, 100, 300 and 500 $Mg(TMHD)_2$-O_3 ALD cycles at 250 °C. The interparticle distance (D) is obtained from the data in Figures 5a-c by applying the relation $D = 2\pi/q_{y,max}$.

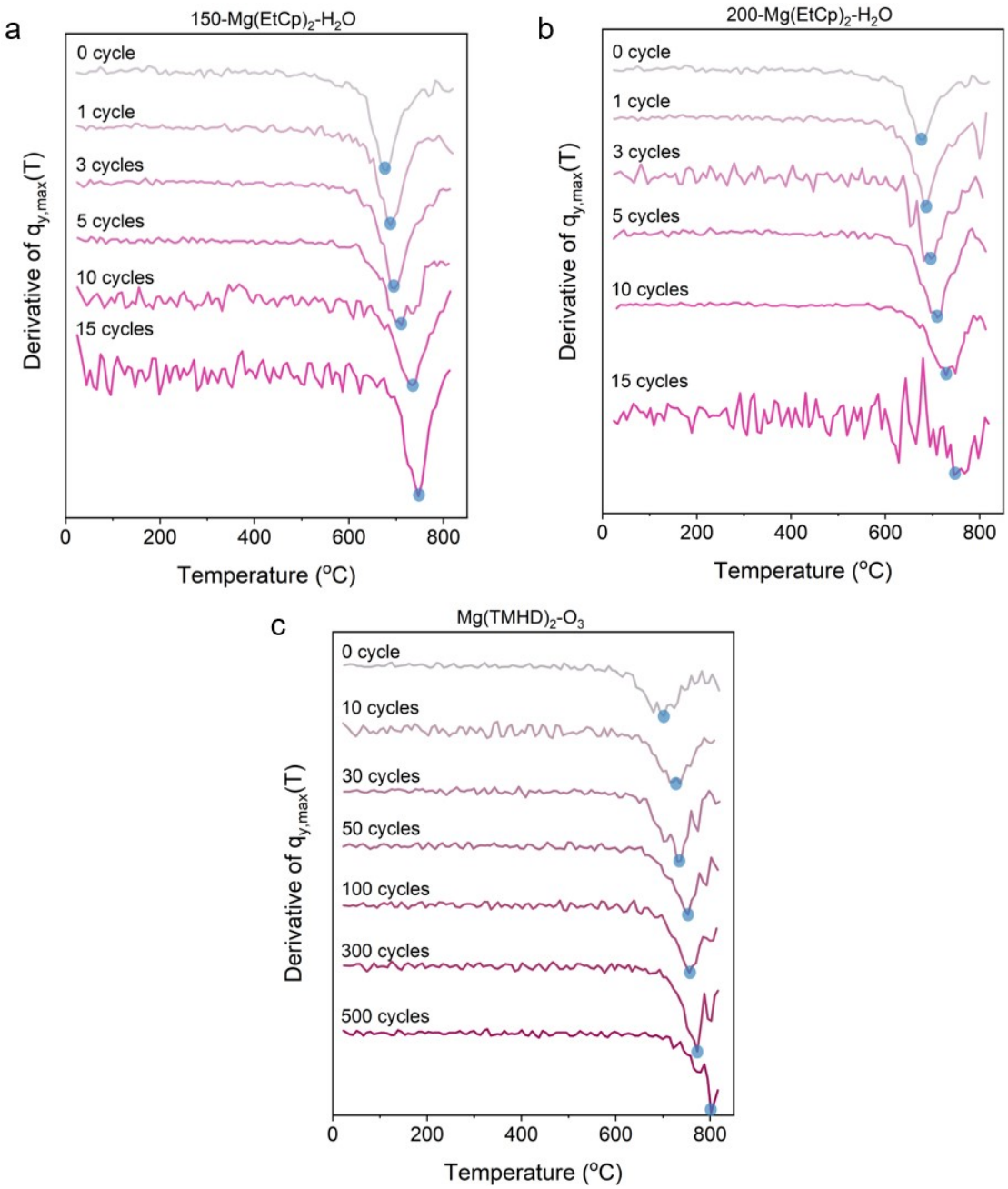

Figure S18. First derivative of the $q_{y,max}$ vs. temperature curves in Figure 5a-c, showing a distinct minimum marked by the blue dots. The temperature at which this minimum occurs, is interpreted as the onset temperature for particle sintering. The onset temperature is plotted as a function of the number of ALD cycles in Figure 5d-f.

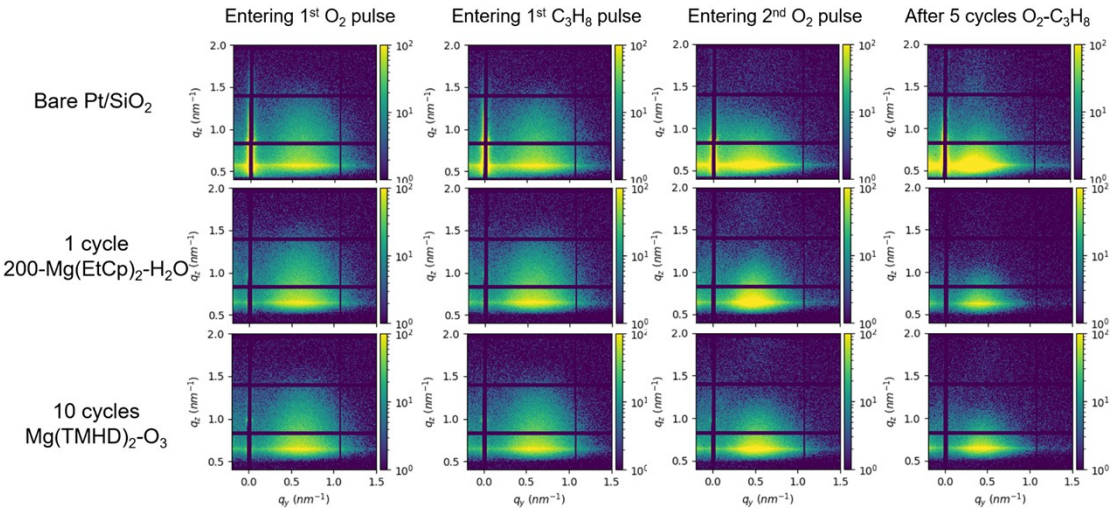

Figure S19. Selection of 2D in-situ GISAXS patterns recorded during five cycles of propane dehydrogenation reaction and reactivation in O_2 (20% O_2 in He) of bare Pt/SiO_2 and two MgO-coated Pt/SiO_2, one synthesized with 1 $Mg(EtCp)_2$-H_2O ALD cycle at 200 °C and one synthesized with 10 $Mg(TMHD)_2$-O_3 ALD cycles at 250 °C.

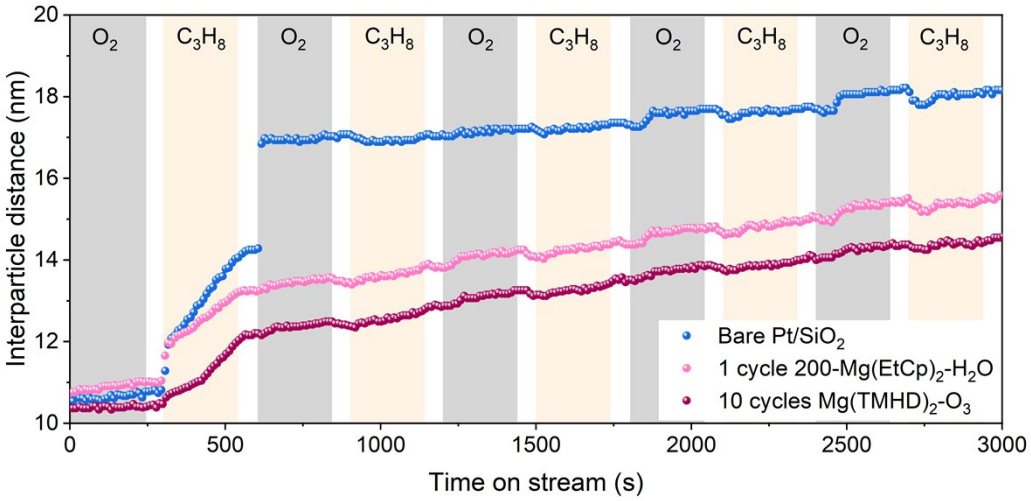

Figure S20. The evolution of interparticle distance during five cycles of propane dehydrogenation reaction (5% C_3H_8 in He) and regeneration in O_2 (20% O_2 in He) at 600 °C, showing the evolution NPs spacing with time for three samples: bare Pt/SiO_2 and two MgO-coated Pt/SiO_2, one synthesized with 1 $Mg(EtCp)_2$-H_2O ALD cycle at 200 °C and one synthesized with 10 $Mg(TMHD)_2$-O_3 ALD cycles at 250 °C. The values are calculated from the in-situ record of $q_{y,max}$ values.